A Novel Control DC-DC-AC Buck Converter for Single Phase Capacitor-Start-Run Induction Motor Drives

Gerald Chidozie DIYOKE[1], *Cosmas Uchenna OGBUKA*[2], *Cajethan Maduabuchi NWOSU*[2]

[1]Department of Electrical & Electronic Engineering, College of Engineering and Engineering Technology, Michael Okpara University of Agriculture, Umuahia - Ikot Ekpene Road, Umudike, Abia State, Nigeria
[2]Department of Electrical Engineering, Faculty of Engineering, University of Nigeria, Nsukka Road, 410001 Nsukka, Enugu State, Nigeria

geraldiyoke@mouau.edu.ng, cosmas.ogbuka@unn.edu.ng, cajethan.nwosu@unn.edu.ng

DOI: 10.15598/aeee.v17i2.2904

Abstract. *A novel control DC-DC-AC buck converter for single phase capacitor-start-run induction motor drives is presented in this paper. The objective is to minimize harmonic distortion in inverter output voltage supply to a Single Phase Induction Motor (SPIM). Here, the output of a variable duty cycle buck DC-DC converter is fed to an H-bridge inverter to generate a very close sinusoidal output voltage. Few power semiconductor switches are utilized to produce inverter output voltage with reduced harmonic distortion comparable with results achieved in multilevel inverters. The SPIM was analysed in the stationary d-q reference frame while the buck converter was operated in the Continuous Conduction Mode (CCM) to ensure that the output voltage vary exactly as the duty cycle. The simulation results show good starting transient characteristics for the SPIM and also stable operation under intermittent loading of 4 N-m. The average inverter output voltage of 157.4 V was achieved with Total Harmonic Distortion (THD) as low as 6.32 %. This configuration is simple, cheap, and has reduced control complexity.*

Keywords

Capacitor start-run, DC-DC buck converter, duty cycle, induction motor, inverter, single-phase.

1. Introduction

The quality of inverter voltage supply to electrical loads has attracted considerable research attention in recent years. Specific attention has been devoted to the problem of harmonic distortion in inverter output voltage [1], [2], [3], and [4]. Efficient operation of Single Phase Induction Motors (SPIM), for industrial and domestic applications, depend on the harmonic content of inverter output voltage [5], [6], [7], [8], and [9].

Several multilevel inverter topologies have been proposed in literature to minimize harmonics distortions in inverter output voltages [10], [11], [12], and [13]. For instance, a circuit configuration with a novel control algorithm for the DC-DC buck converter, which results in an n-level multilevel inverter output voltage, was presented in [14]. In this work, tabulated results of percentage THD for different inverter output levels are shown for simulation and experimentation. The 3 level inverter has percentage THD of 45.38 and 45.6 for simulation and experimentation, respectively. On the other hand, the 255 level inverter has percentage THD of 0.37 and 1.4 for simulation and experimentation, respectively. This clearly shows that an increase in the inverter output voltage levels results in reduction of the THD.

It was, however, observed that power loss in the circuit increases with increase in the number of output voltage levels. Consequently, the inverter efficiency decreases with increase in the number of levels in output AC voltage. Apart from high switching losses (leading to reduction in efficiency), multilevel inverter topologies also have other demerits, including complexity in the generation of control signals, high number of circuit components, and high weight [15], [16], and [17].

The interface between the inverters and unregulated DC sources such as electromechanical DC generators, batteries, rectified AC source, solar photovoltaic panels or hydrogen based fuel cells are the DC-DC converters

[18], and [19]. There are six types of basic DC-DC converter with each having performance characteristic suitable for a particular application. These basic types are the step down or buck converter, the step up or boost converter, the conventional buck-boost converter, the Cuk's, the Sepic, and the Zeta converters [20], [21], [22], and [23].

In this paper, a novel control DC-DC-AC buck converter for single phase capacitor-start-run induction motor drives is presented. A fundamental frequency rectified sine reference signal with a high frequency carrier signal placed above zero reference modulation technique is adopted. An H-bridge inverter topology with fundamental frequency control is used to invert the buck DC-DC output voltage. The research objective is to obtain inverter AC output voltage with reduced THD comparable with results obtained using multilevel inverters while employing reduced number of power semiconductor switches to offer excellent transients and steady state performance of the motor. The software for the research is MATLAB/Simulink 2014a version.

The organization of this paper is such that the circuit description and operation of DC-DC-AC conventional inverter is presented in Sec. 2. Simulation of the proposed complete circuit topology, result presentation and discussion are carried out in Sec. 3. The work is concluded in Sec. 4.

2. Circuit Description and Operation

The circuit diagram of the proposed inverter topology is shown in Fig. 1, in which a DC-DC buck converter is coupled with a conventional H-bridge inverter. In the half cycle, S1 and S2 are turned ON, thereby allowing the half waveform from the buck converter to appear at the inverter output. Furthermore, in the subsequent half cycle, S3 and S4 are turned ON, thereby inverting the second waveform from the buck output voltage. The two resultant waveforms gave a sinusoidal waveform as depicted in Fig. 1. The power semiconductor switch S, can be a single high voltage and current switch or series high current or low voltage switches, which can meet the necessary full Vdc hold-off requirement. The advent of Insulated Gate Bipolar Transistor (IGBT) has made important contribution to power electronics because the power and frequency boundaries have been extended. Inverter circuits for motor drives are predominantly made of IGBTs. The relationship between the input and output voltages is related by the duty cycle.

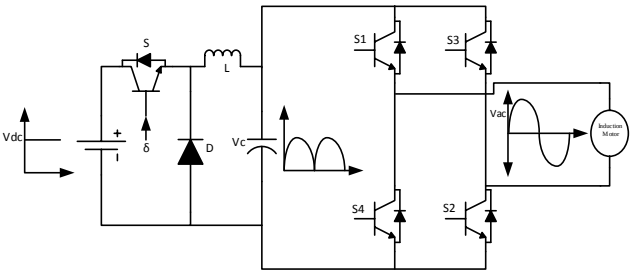

Fig. 1: Circuit diagram of the proposed inverter configuration.

2.1. Generation of Variable PWM Duty Cycle

A method of varying duty cycle of DC-DC converter is obtained by comparing the reference signal (rectified sine wave) and carrier triangular signal (placed above zero level). An array of PWM signal generated comprises of unequal intervals between 0–90° and 90–0°, which represents the variation of sine function which has a minimum value at zero degree and maximum at 90 degrees. Sine-triangle carrier modulation is identified as the most promising technique to pursue for both technical and pedagogical reasons [24], and [25].

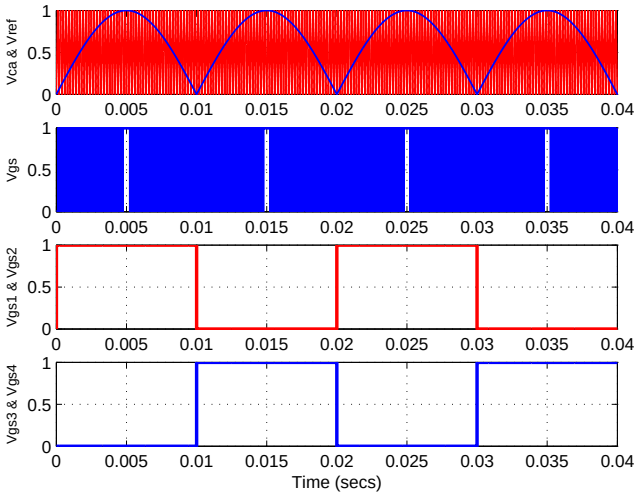

Fig. 2: Carrier and rectified signals and corresponding switching pulses.

Figure 2 shows the generation of PWM control signal, V_{gs}, for firing the switch S of Fig. 1. This is obtained by comparing a carrier and a reference signal. Also shown in Fig. 2 are the firing pulses V_{gs1}–V_{gs4} for the H-bridge inverter switches S1-S4 generated by comparing the reference signal with ground potential. The block diagram for the generation of these firing pulses is shown in Fig. 3.

Figure 2 shows the generation of PWM control signal, V_{gs}, for firing the switch S of Fig. 1. This is obtained by comparing a carrier and a reference signal. Also shown in Fig. 2 are the firing pulses V_{gs1}–V_{gs4}

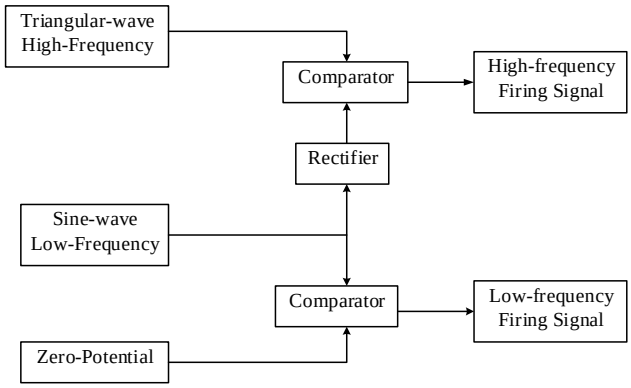

Fig. 3: Logic circuit configuration for corresponding switching pulses.

for the H-bridge inverter switches S1–S4 generated by comparing the reference signal with ground potential. The block diagram for the generation of these firing pulses is shown in Fig. 3.

2.2. Design of Buck Converter Parameters

The Buck converter is operated in Continuous Current Mode (CCM) to enable the output voltage, V_o, to exactly follow the duty cycle variation. The procedure for the design of buck converter with the given specifications of: DC input voltage, V_{dc}, capacitor average current, V_{Cavg}, minimum output current, $I_{o\,\min}$, maximum output current, $I_{o\,\max}$, switching frequency, f_s and duty cycle, δ (Reference signal voltage, V_{ref}/Carrier signal voltage, V_{ca}) ≤ 1 % is described in [21], [22], and [24].

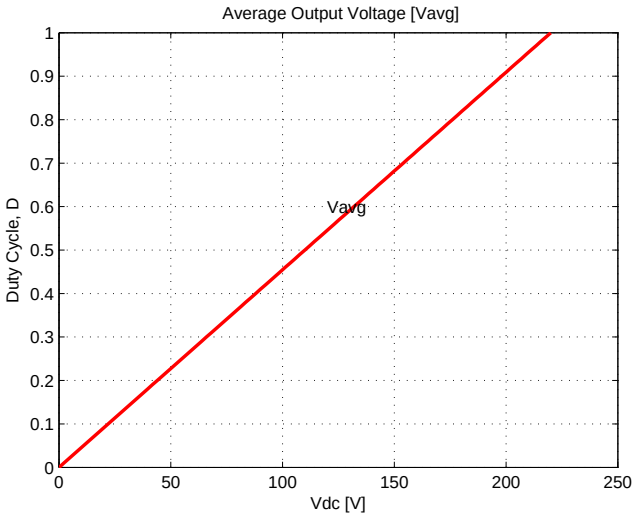

Fig. 4: Duty cycle vs. output voltage plot for a constant input voltage.

The linear relationship existing between the input voltage and output voltage of the DC-DC buck converter shown in Fig. 4 makes it possible to realize a rectified output voltage for the buck converter. The duty cycle and the other converter parameters are computed as in [14], [20], and [26].

Tab. 1: Parameters of the converter.

Specifications	DC Input Voltage V_{dc}	220 V
	Minimum Output Current $I_{o\,\min}$	0.2 A
	Maximum Output Current $I_{o\,\max}$	10 A
	Switching frequency f_s	5 kHz
	Fudamental Frequency FF	50 Hz
Designed parameters	Inductance L	1 mH
	Capacitance C	47 µF

2.3. D-Q Modelling of Capacitor Start Capacitor Run Induction Motor

To achieve good steady state performance and high starting torque, two capacitors are used in a variant of the capacitor-start-run motor shown in Fig. 5. To start the motor, a relatively large capacitor value is used for high starting torque. This is followed by the application of a low value capacitor to sustain staedy state operation without excessive current. Thus, the motor combines the advantages of capacitor-run and capacitor-start motors (i.e. good running power factor, efficiency, quiet and smooth operation, and high starting torque). Typical applications are refrigerators, compressors, conveyers, air conditioners, or pumps.

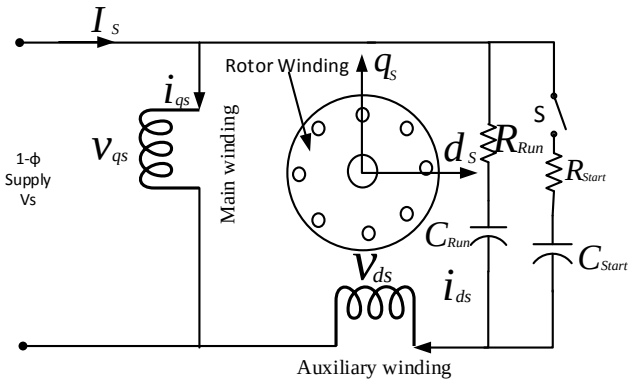

Fig. 5: Capacitor-start capacitor-run induction motor.

The equivalent circuit model is obtained in [8], thus the modified machine input voltage for single phase capacitor-start capacitor-run induction motor is modelled as follows:

$$V_{qs} = V_s = V_{ac}. \tag{1}$$

The equivalent impedance Z_{eq} of the start-run capacitor is given by:

$$\begin{aligned} Z_{eq} &= (R_{run} + jXC_{run})//(R_{start} + jXC_{start}) \\ &= Z_{run}//Z_{start}. \end{aligned} \tag{2}$$

During start, the switch S is turned ON thereby connecting the capacitor-start, thus we have:

$$V_{ds} = V_s - \frac{1}{Z_{eq}} \int i_{ds} \mathrm{d}t. \tag{3}$$

At 75 % synchronous speed, the switch S turns OFF thereby disconnecting capacitor start, thus we get:

$$V_{ds} = V_s - \frac{1}{Z_{run}} \int i_{ds} \mathrm{d}t, \tag{4}$$

$$V_{qs} = i_{ds} R_{ds} + p\lambda_{ds} - \omega_r \lambda_{qs}, \tag{5}$$

$$V_{ds} = i_{qs} R_{qs} + p\lambda_{qs} - \omega_r \lambda_{ds}, \tag{6}$$

$$V_{dr} = i_{dr} R_{dr} + p\lambda_{dr}, \tag{7}$$

$$V_{qr} = i_{qr} R_{qr} + p\lambda_{qr}, \tag{8}$$

$$P\omega_r = \frac{T_e}{J} - \frac{T_L}{J} - \frac{B_m}{J}\omega_r, \tag{9}$$

where:

- λ_{dr} and λ_{qr} are the d-axis, and q-axis, rotor flux linkages,
- λ_{ds} and λ_{qs} are the d-axis, and q-axis, stator flux linkages,
- R_{start} and C_{start} are resistance start and Capacitor-Start,
- R_{run} and C_{run} are resistance-run and Capacitor-Run,
- Z_{start} and Z_{run} are start and run impedances,
- V_{qs} and i_{qs} are q-axis main winding voltage and current,
- V_{ds} and i_{ds} are d-axis auxiliary winding voltage and current,
- V_{qr} and i_{qr} are q-axis rotor voltage and current,
- V_{dr} and i_{dr} are d-axis rotor voltage and current,
- $V_s = V_{ac}$ is the inverter output voltage,
- $p = \frac{\mathrm{d}}{\mathrm{d}t}$ is differential operator,
- P is number of pole pairs,
- ω_r is the mechanical rotational speed,
- T_L is load Torque, T_e is electromagnetic Torque,
- J is load inertia coefficient,
- B_m is damping coefficient.

3. Simulation, Results, and Discussion

Figure 6 shows the complete schematic of the proposed single phase capacitor-start capacitor-run induction motor drives. It comprises the DC-DC buck converter operating in continuous current conduction mode at a variable duty cycle; a conventional DC-AC inverter with four power switches operating at a low frequency of 50 Hz; and a coupled load of single phase capacitor start capacitor run induction machine.

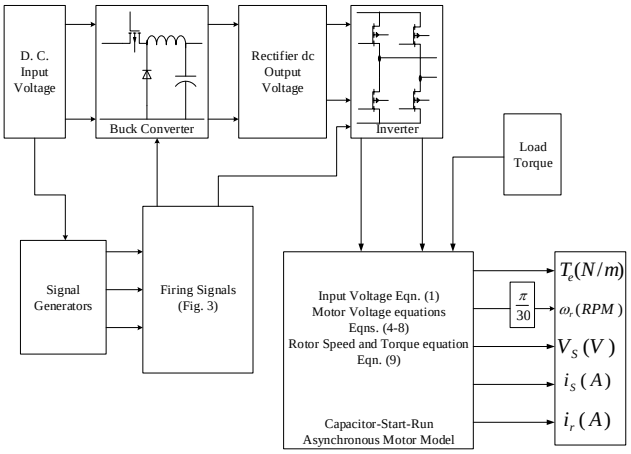

Fig. 6: Complete schematic of the single phase capacitor-start capacitor-run induction motor drives.

The circuit configuration shown in Fig. 1 along with the method for varying duty cycle shown in Fig. 3 has been simulated in MATLAB/Simulink and the results shown in Fig. 2. The specifications considered for the design of filter parameters of DC-DC converter and the values of L and C obtained from the aforementioned design procedure are tabulated in Tab. 1. Figure 4 depicts duty cycle versus input voltage plot, which shows the linear relationship between the three vital buck converter parameters.

Figure 7 and Fig. 8 depict DC-DC buck converter voltages and currents plots. It is clear from Fig. 7 that with the designed parameters, the output DC-DC converter, V_o exactly followed the duty cycle variation. In

addition, the inductor voltage was also plotted and it shows a variation which is a function of duty cycle. Figure 8 depicts inductor current which operates at the boundary condition of continuous and discontinuous conduction current modes which depends on duty cycle, switching frequency and inductor value. In addition, the DC-DC buck converter output current was also plotted and the result depends on the variation of the duty cycle. Figure 9 shows the inverter output voltage.

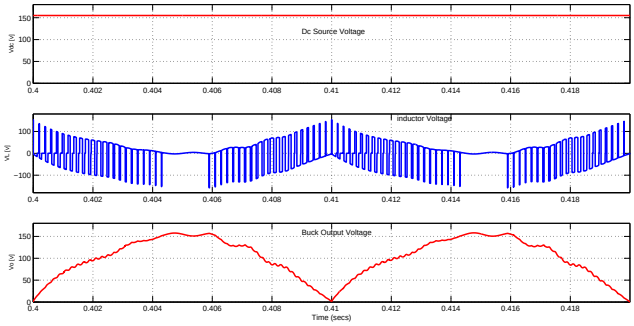

Fig. 7: Buck converter waveforms for DC source, inductor and output voltages.

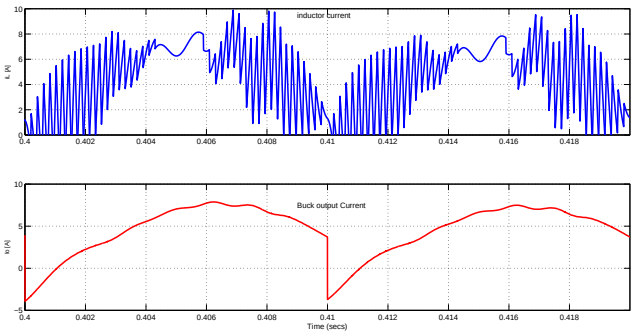

Fig. 8: Buck converter waveforms for inductor and output currents.

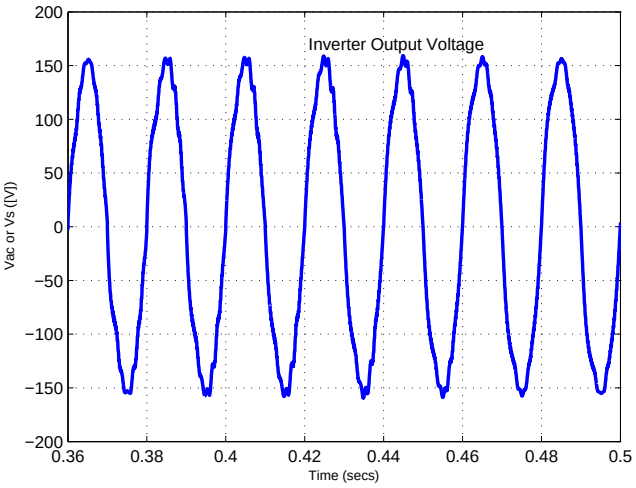

Fig. 9: Inverter output voltage waveform.

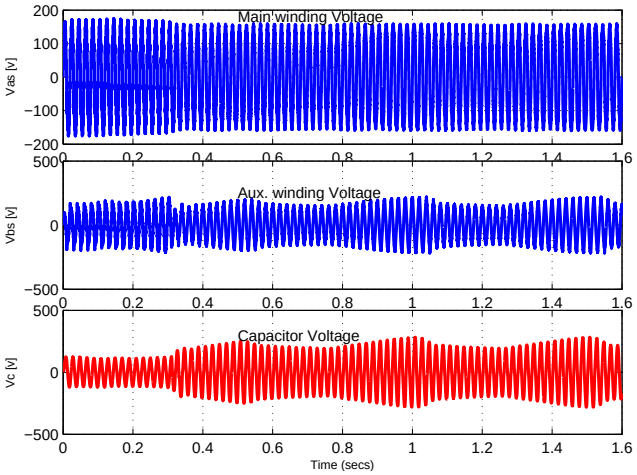

Fig. 10: Capacitor-start capacitor-run induction machine voltage waveforms.

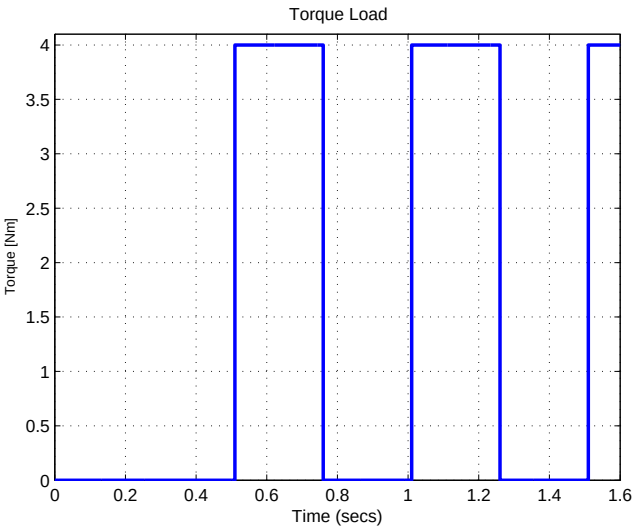

Fig. 11: Machine loading profile.

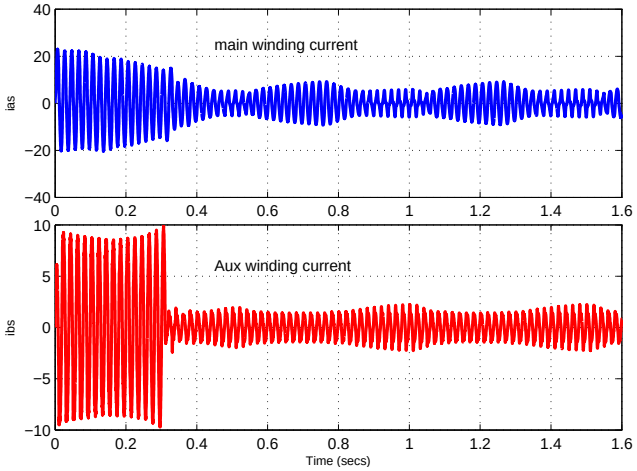

Fig. 12: Capacitor-start capacitor-run induction machine output current waveforms.

The inverter output voltage (i.e. main winding voltage), the auxiliary winding voltage, and the capacitor-

start-run voltages are shown in Fig. 10. This confirms that the proposed circuit configuration in Fig. 1 is capable of producing sinusoidal AC voltage using one DC source few semiconductor switches.

The loading sequence for the machine is shown in Fig. 11. The machine was loaded with 4 Nm at 0.51 seconds until 0.76 seconds when the load was removed (a period of 0.25 seconds). It was loaded again at 1.01 seconds (0.25 seconds later) and sustained for another 0.25 seconds before the load was removed at 1.26 seconds. Thus, an equal interval of 0.25 seconds for load and offload was maintained. The effect of the loading sequence is observed in Fig. 10, Fig. 12, and Fig. 13. Figure 12 shows the main winding current and auxiliary winding current, from which the main winding inrush current or starting current is little above 20 A while that of auxiliary winding is little below 10 A.

The dynamic waveforms of the induction motor are obtained in Fig. 13, which depict the following plots; Electromagnetic torque under 4 N-m load torque, rotor speed running at 1500 rpm maximum and 1300 rpm minimum speed, and torque-speed which shows the behaviour of torque at different rotor speed values. The effect of the 4 Nm intermittent loading can be noticed in the electromagnetic torque, rotor speed, and torque-speed plots. Figure 14 shows the phase-plane portrait of the system, displaying the periodicity of the capacitor-start capacitor-run motor. Figure 14 depicts the rotor currents in D-Q axes plots. These oscillations are caused by elliptical rotating field due to the phase difference between the rotor currents in D-Q-axes and also unequal amplitudes of these currents.

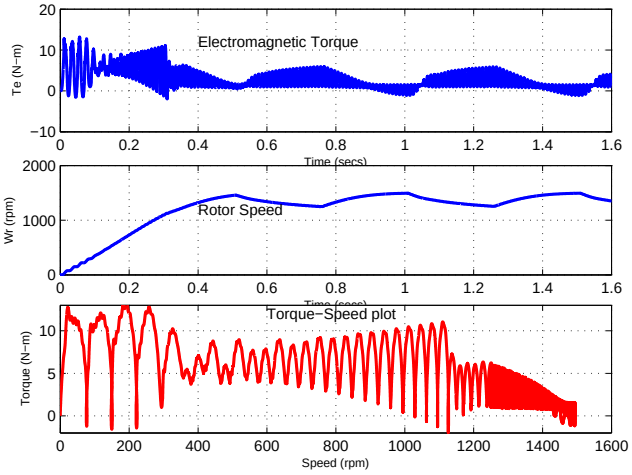

Fig. 13: Waveforms for electromagnet torque, rotor speed and torque vs. speed plots.

The harmonic spectrum for the machine input voltage is shown in Fig. 15 above. The spectrum displays the operating frequency of the machine (50 Hz), average input voltage (157.4 V) and THD of 6.32 %.

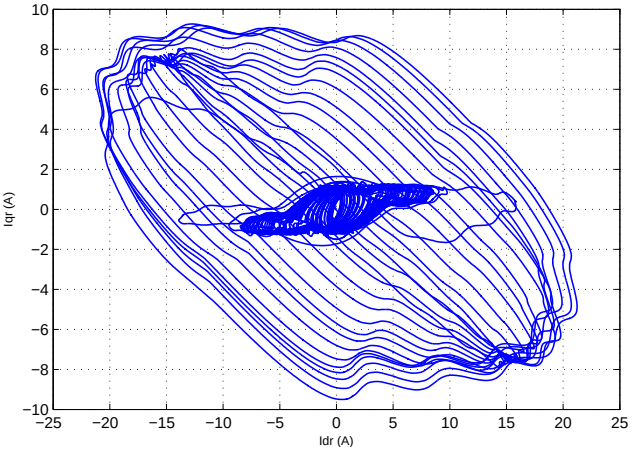

Fig. 14: Trajectory of the rotor currents i_{qr} versus i_{dr}.

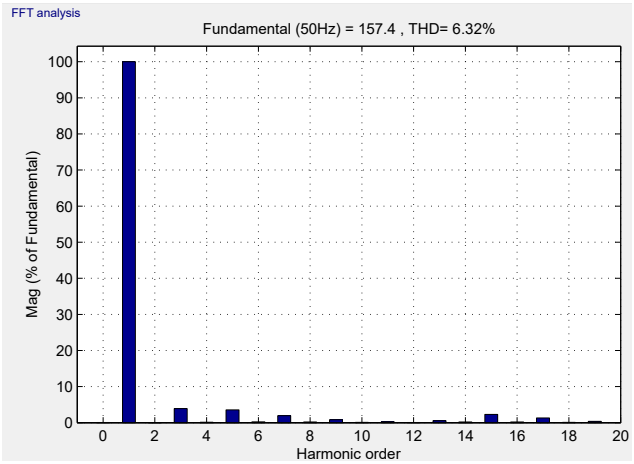

Fig. 15: Inverter output voltage FFT analysis.

4. Conclusion

A voltage source inverter with single DC source and reduced number of power components, which can generate voltage very close to a pure sinusoidal wave with a variable duty cycle, was presented. This circuit configuration along with a novel DC-DC control technique results in reduced control complexity, lower switching losses, lower cost and weight, and higher efficiency. Above all, the single phase induction motor exhibited excellent dynamic performance during sudden gain, loss of load, and enhanced starting torque. From the results, it is concluded that the proposed DC-DC buck control method performs very effectively in producing an output AC voltage very close to sinusoidal waveform with THD reduced to as low as 6.32 % using a single DC voltage source and employing reduced number of power semiconductor switches. This result is comparable with the results of multilevel inverters which have inherent limitation of increased power loss, reduced efficiency, complexity in the generation of control signals, high number of circuit components, and high weight.

References

[1] WANG, Y., X. WANG and D. GERLING. A Precise Voltage Distortion Compensation Strategy for Voltage Source Inverters. *IEEE Transactions on Industrial Electronics*. 2018, vol. 65, iss. 1, pp. 59–66. ISSN 0278-0046. DOI: 10.1109/TIE.2017.2716866.

[2] VOVOS, N. A., P. N. VOVOS and K. G. GEORGAKAS. Harmonic Reduction Method for a Single-Phase DC-AC Converter without an Output Filter. *IEEE Transactions on Power Electronics*. 2014, vol. 29, iss. 9, pp. 4624–4632. ISSN 0885-8993. DOI: 10.1109/TPEL.2013.2286918.

[3] KAPOOR, P. and M. RENGE. Improved Performance of Modular Multilevel Converter for Induction Motor Drive. *Energy Procedia*. 2017, vol. 117, iss. 1, pp. 361–368. ISSN 1877-7058. DOI: 10.1016/j.egypro.2017.05.146.

[4] BARTMAN, J. Analysis of Output Voltage Distortion of Inverter for Frequency Lower than Nominal. *Journal of Electrical Engineering*. 2017, vol. 68, iss. 3, pp. 194–199. ISSN 1335-3632. DOI: 10.1515/jee-2017-0028.

[5] DARBALI-ZAMORA, R., D. A. MERCED-CIRINO, A. J. DIAZ-CASTILLO and E. I. ORTIZ-RIVERA. Single phase induction motor alternate start-up and speed control method for renewable Energy application. In: *International conference on Renewable Energy Research and Application (ICRERA)*. Milwaukee: IEEE, 2014, pp. 743–748. ISBN 978-1-4799-3795-0. DOI: 10.1109/ICRERA.2014.7016484.

[6] HANAFY, H. Dynamic Analysis of a New Connection for Dual Voltage Operation of Single Phase Capacitor Run Motor. *Journal of Electrical Engineering*. 2013, vol. 13, iss. 1, pp. 1–8. ISSN 1582-4595.

[7] OJAGHI, M. and S. DALIRI. Analytic Model for Performance Study and Computer-Aided Design of Single-Phase Shaded-Pole Induction Motors. *IEEE Transactions on Energy Conversion*. 2017, vol. 32, iss. 2, pp. 649–657. ISSN 0885-8969. DOI: 10.1109/TEC.2016.2645641.

[8] LEICHT, A. and K. MAKOWSKI. Analysis of a Single-Phase Capacitor Induction Motor Operating at Two Power Line Frequencies. *Archives of Electrical Engineering*. 2012, vol. 61, iss. 2, pp. 251–266. ISSN 1427-4221. DOI: 10.2478/v10171-012-0021-3.

[9] JANNATI, M., S. ANBARAN, S. ASGARI, W. GOH and N. IDRIS. A Review on Variable Speed Control Techniques for Efficient Control of Single-Phase Induction Motors: Evolution, Classification, Comparison. *Renewable and Sustainable Energy Reviews*. 2017, vol. 75, iss. 1, pp. 1306–1319. ISSN 1364-0321. DOI: 10.1016/j.rser.2016.11.115.

[10] ABDALLA, I., J. CORDA and L. ZHANG. Multilevel DC-Link Inverter and Control Algorithm to Overcome the PV Partial Shading. *IEEE Transaction on Power Electronics*. 2013, vol. 28, iss. 1, pp. 14–18. ISSN 0885-8993. DOI: 10.1109/TPEL.2012.2209460.

[11] HAMZEH, M., A. GHAZANFARI, H. MOKHTARI and H. KARIMI. Integrating Hybrid Power Source into an Islanded MV Microgrid using CHB Multilevel Inverter under Unbalanced and Nonlinear Load Conditions. *IEEE Transaction on Energy Conversion*. 2013, vol. 28, iss. 3, pp. 643–651. ISSN 0885-8969. DOI: 10.1109/TEC.2013.2267171.

[12] POURESMAEIL, E., D. MONTESINOS-MIRACLE and O. GOMIS-BELLMUNT. Control Scheme of Three-Level NPC Inverter for Integration of Renewable Energy Resources into AC Grid. *IEEE Systems Journal*. 2012, vol. 6, iss. 2, pp. 242–253. ISSN 1932-8184. DOI: 10.1109/JSYST.2011.2162922.

[13] LI, J., J. LIU, D. BOROYEVICH, P. MATTAVELLI and X. YAOSUO. Three Level Active Neutral-Point Clamped Zero-Current-Transition Converter for Sustainable Energy Systems. *IEEE Transaction on Power Electronics*. 2011, vol. 26, iss. 12, pp. 3680–3693. ISSN 0885-8993. DOI: 10.1109/TPEL.2011.2161890.

[14] DASTAGIRI, B., N. ANISH and M. SELVAN. Embedded Control of n-level DC - DC - AC Inverter. *IEEE Transactions on Power Electronics*. 2015, vol. 30, iss. 7, pp. 3703–3711. ISSN 0885-8993. DOI: 10.1109/TPEL.2014.2341245.

[15] LEON, J. I., S. VAZQUEZ and L. G. FRANQUELO. Multilevel Converters: Control and Modulation Techniques for their Operation and Industrial Applications. *Proceedings of the IEEE*. 2017, vol. 105 , iss. 11, pp. 2066–2081. ISSN 1558-2256. DOI: 10.1109/JPROC.2017.2726583.

[16] FRANQUELO, L., J. RODRIGUEZ, J. LEON, S. KOURO, R. PORTILLO and M. PRATS. The Age of Multilevel Converters Arrives. *IEEE Industrial Electronics Magazine*. 2008, vol. 2. iss. 2, pp. 28–39. ISSN 1932-4529. DOI: 10.1109/MIE.2008.923519.

[17] BABAEI, E., S. LAALI and S. BAHRAVAR. A New Cascaded Multi-level Inverter Topology with Reduced Number of Components and Charge Balance Control Methods Capabilities. *Electric Power Components and Systems*. 2015, vol. 43, iss. 19, pp. 2116–2130. ISSN 1532-5008. DOI: 10.1080/15325008.2015.1077485.

[18] FOROUZESH, M., Y. SIWAKOTI, S. A. GORJI and F. BLAABJERG. Step-Up DC-DC Converters: A Comprehensive Review of Voltage Boosting Techniques, Topologies, and Applications. *IEEE Transactions on Power Electronics*. 2017, vol. 32, iss. 12, pp. 9143–9178. ISSN 0885-8993. DOI: 10.1109/TPEL.2017.2652318.

[19] DUONG, T. D. Isolated Boost DC-DC Converter With Three Switches. *IEEE Transactions on Power Electronics*. 2018, vol. 33, iss. 2, pp. 1389–1398. ISSN 0885-8993. DOI: 10.1109/TPEL.2017.2679029.

[20] BUBOVICH, A. The Comparison of Different Types of DC-DC Converters in terms of Low-Voltage Implementation. In: *5th IEEE Workshop on Advances in Information, Electronic and Electrical Engineering (AIEEE)*. Riga: IEEE, 2017, pp. 1–4. ISBN 978-1-5386-4137-8. DOI: 10.1109/AIEEE.2017.8270560.

[21] OGBUKA, C. and G. DIYOKE. Analysis of Switch Mode DC to DC Power Regulators. *International Journal of IEEE Nigeria Section*. 2011, vol. 1, iss. 1, pp. 53–56. ISSN 0978-3038.

[22] AJAMI, A., H. ARDI and A. FARAKHOR. Design, Analysis and Implementation of a Buck-Boost DC/DC Converter. *IET Power Electronics*. 2014, vol. 7, iss. 12, pp. 2902–2913. ISSN 1755-4535. DOI: 10.1049/iet-pel.2013.0874.

[23] LINDIYA, A., S. PALANI and D. BIYYAPPANA. Performance Comparison of Various Controllers for DC-DC Synchronous Buck Converter. *Procedia Engineering*. 2012, vol. 38, iss. 1, pp. 2679–2693. ISSN 1877-7058. DOI: 10.1016/j.proeng.2012.06.315.

[24] ANDRADE, M. and V. COSTA. DC-DC Buck Converter with Reduced Impact. *Procedia Technology*. 2014, vol. 17, iss. 1, pp. 791–798. ISSN 2212-0173. DOI: 10.1016/j.protcy.2014.10.209.

[25] RAKESH, P. and G. NARAYANAN. Analysis of Sine-Triangle and Zero-Sequence Injection Modulation Schemes for Split-Phase Induction Motor Drive. *IET Power Electronics*. 2016, vol. 9, iss. 2, pp. 344–355. ISSN 1755-4535. DOI: 10.1049/iet-pel.2015.0066.

[26] KIMBALL, J. and M. ZAWODNIOK. Reducing Common-Mode Voltage in Three-Phase Sine-Triangle PWM with Interleaved Carriers. *IEEE Transactions on Power Electronics*. 2011, vol. 26, iss. 8, pp. 2229–2236. ISSN 0885-8993. DOI: 10.1109/TPEL.2010.2092791.

About Authors

Gerald Chidozie DIYOKE was born in Aku Nigeria on 9th October, 1980. He received his B.Eng. (Second Class Upper Honors), and M.Eng. (Distinction) from the Department of Electrical Engineering, University of Nigeria Nsukka (UNN) in 2005 and 2013, respectively. He is currently a Ph.D. student in the Department of Electrical Engineering UNN and a Lecturer at the Department of Electrical and Electronic Engineering, Michael Okpara University of Agriculture, Umudike, Abia, Nigeria. His research interests are Power electronics, conventional and multilevel inverter, Induction motor drives.

Cosmas Uchenna OGBUKA was born in Umuna Nigeria on 1st April, 1981. He holds the following degrees from the Department of Electrical Engineering, University of Nigeria Nsukka, where he has attained the rank of Senior Lecturer: B.Eng. (First Class Honors), M.Eng. (Distinction) and Doctor of Philosophy (Ph.D.) obtained in 2004, 2009, and 2014 respectively. His research interests include Electrical Machines, Drives and Power Electronics. He is currently an International Faculty Fellow at the Massachusetts Institute of Technology, Cambridge Massachusetts USA having recently (February 2017 to May 2017) concluded the MIT-ETT Fellowship under MIT International Science and Technology Initiative (MISTI-AFRICA). He previously (November 2015 to April 2016) undertook a postdoctoral research visit at the Chair of Electrical Drives and Actuators (EAA) Universitaet der Bundeswehr Muenchen Germany. He is the corresponding author for this manuscript.

Cajethan Maduabuchi NWOSU was born 1st October 1967. He obtained the B.Eng, M.Eng, and Ph.D. Degrees in Electrical Engineering from the University of Nigeria, Nsukka in 1994, 2004, and 2015 respectively. In 2007, he undertook a three months pre-doctoral research on Wind/Solar Hybrid Power System and Renewable Energy Resources at the University of Technology, Delft (TU-Delft), the Netherlands. Since 2005, he has been with the Department of Electrical Engineering, University of Nigeria, Nsukka, where he is currently a Senior Lecturer. He had written two books and had published over thirty articles both in local and international journals. He is an executive member of Nigerian Institution of

Electrical and Electronic Engineers (NIEEE), Nsukka chapter. He is a member of Power Electronics Society of Institution of Electrical and Electronic Engineering (PES IEEE). He is an editorial board member World Science Journal of Engineering Applications. His areas of research interest include power electronic converters, electrical drives and renewable energy technologies.

Appendix A
Single Phase Induction Motor Parameters

- Rated Voltage (V) = $110\sqrt{2}$.
- Rated Power (Hp) = 1/4.
- Frequency (Hz) = 50.
- Number of Pole pairs = 2.
- Rated Speed (RPM) = 1500.
- Inertia (kg·m^2) = 0.0146.
- Friction factor (N·m·s) = 0.
- Turn ratio (aux/main) = 1.18.
- Main winding stator [R_s (Ω), L_{Is}]=2.02, $7.4{\cdot}10^{-3}$.
- Main winding stator [R'_r (Ω), L'_{Ir}]=4.12, $5.6{\cdot}10^{-3}$.
- Main winding Mutual Inductance L_{ms} (H)=0.1772.
- Auxiliary winding stator [R_s (Ω), L_{ls} (H)] = 7.14, $85 \cdot 10^{-3}$.
- Capacitor-start [R_{st} (Ω), C_s (Farad)] = 2, $254.7 \cdot 10^{-6}$.
- Capacitor-run [R_{ru} (Ω), C_{ru} (Farad)] = 18, $21.1 \cdot 10^{-6}$.